

# Strong four-phonon processes on thermal conductivity of two-dimensional materials in the low-temperature region

H. F. Feng, B. Liu, and Zhi-Xin Guo\*

*State Key Laboratory for Mechanical Behavior of Materials, Center for Spintronics and Quantum System, School of Materials Science and Engineering, Xi'an Jiaotong University, Xi'an, Shanxi, 710049, China.*

\*[zxguo08@xjtu.edu.cn](mailto:zxguo08@xjtu.edu.cn)

## Abstract

First principles-based predictions of lattice thermal conductivity (TC) from perturbation theory have achieved significant success. In general, it only includes three-phonon (3ph) scattering. However, recent studies have revealed that four-phonon (4ph) scattering, treated under single-mode relaxation time approximation (RTA), has a comparable impact to 3ph scattering at medium and high temperatures in various materials, particularly in two-dimensional (2D) materials. Nonetheless, the influence of 4ph scattering on TC at low temperatures has not been explored so far, owing to the assumption that 4ph processes are generally insignificant at low temperatures. By combining the first-principles calculations, machine learning techniques, Boltzmann transport equation (BTE), and molecular dynamics (MD) simulations, we find that there are unusually strong 4ph processes in the low-frequency range of 2D materials such as h-XN (X=B, Al, Ga), which have remarkable influence on the low-temperature TC. We also find that the strong 4ph processes are originated from the flexural out-of-plane acoustic (ZA) phonon mode of 2D materials. We further discover the remarkable normal (N) processes of 4ph scattering in 2D materials, which make the conventionally adopted perturbation methods for TC calculation far from sufficient at low temperatures. Finally, we find that the intensity of 4ph scattering and thus TC can be effectively manipulated by changing the dispersion of ZA phonon mode, which can be easily achieved through strain engineering. Our study provides new insights into low-temperature phonon transport and its manipulation in 2D materials.

Recently, thermal conductivity (TC) of 2D materials has attracted great attention [1-4]. In contrast to that of 3D materials, the exact experimental measurement of TC in 2D materials has been found to be quite a challenge due to their atomic scale thicknesses. Therefore, the theoretical investigation of TC for 2D materials becomes a hot topic [5,6], among which the first-principles-based BTE approach is one of the most widely used methods. Notably, the BTE method considering only 3ph scattering has achieved remarkable success in calculating the TC of solids [7-9]. Nevertheless, recent studies revealed that only considering 3ph processes is not sufficient for the estimation of TC at medium and high temperatures (especially for the 2D materials), and 4ph scattering must be considered [10-15].

In the treatment of 4ph scattering, the single-mode relaxation time approximation (RTA) is generally employed [16]. It has been found that the inclusion of 4ph scattering at the RTA level leads to a significant decrease of TC at medium and high temperatures, which gives rise to remarkable agreement between the theoretical and experimental results [12,17-19]. While, the influence of 4ph scattering at low temperatures has not been explored so far, since it is generally believed there is a much smaller phonon-scattering probability in the low-temperature region owing to the limited excited phonon modes. Nevertheless, the ZA phonon mode, uniquely existing in 2D materials, usually has a remarkable contribution to TC [20,21]. It is noted that ZA phonon mode normally has very low frequencies, which is expected to have a significant influence on TC even at low temperatures. This feature means that the 4ph processes correlated to ZA mode have to be seriously considered even at low temperatures. Hence, further investigation of the 4ph processes on TC of 2D materials in the low-temperature region is in great need.

To carry out such a study, the analysis of 4ph scattering on TC at low temperatures is crucial. The most effective approach is the first-principles-based BTE method, which has been widely employed for calculating TC in materials. However, it is recognized that this method can effectively consider the phonon transport of 4ph processes only at the RTA level, and it faces challenges in precisely treating the 4ph processes with an iterative scheme (ITA) [16]. On the other hand, although molecular dynamics (MD)

simulations can accurately consider all-order phonon-phonon scatterings (3ph, 4hp, etc.) [22], they suffer from the lack of accurate interatomic potential for dynamic simulations [23,24]. Nevertheless, the emergence of machine learning potential (MLP) method provides a solution to this limitation. MLP employs regression algorithms to determine the *ab-initio* potential energy surface, which makes the accuracy of interatomic potential comparable to that from first-principle calculations based on the density functional theory (DFT) [25-27]. Hence, TC obtained from the MLP-based MD simulations can be recognized as a reliable reference for exploring the 4ph processes beyond the RTA level.

In this work, by combining the first-principles calculations [28-30], MLP method [31-33], Boltzmann transport equation (BTE) [16,34-36], and MD simulations [37-39], we discover the unusually large 4ph processes in the low-temperature region of 2D materials, i.e., h-XN (X=B, Al, Ga) monolayers. We find that the ZA phonon mode in 2D materials gives rise to strong 4ph processes and thus induces a large reduction of TC in the low-temperature region. We additionally find that the commonly adopted perturbation methods, i.e., treating 3ph scattering with an iterative scheme beyond RTA and the 4ph scattering at the RTA level, are far from sufficient in the low-temperature region. Based on the influence of ZA mode on 4ph scattering, the 4ph scattering intensity and thus TC can be effectively manipulated by strain engineering.

The nitrogen-based III–V monolayers of h-XN (X=B, Al, Ga), with a typical 2D hexagonal structure like graphene, are ideal candidates for this study. Note that, the h-XN monolayers have very similar geometry but significantly distinct phonon dispersions due to the different atomic mass X. Hence, a systemic investigation of the influence of 4ph processes on TC in the low-temperature region can be achieved via the study on the h-XN system.

We first perform the DFT calculations on the atomic structures and phonon dispersions of h-XN (X=B, Al, Ga) monolayers. As shown in Figs. 1(a)-1(c), all three h-XN monolayers possess a 2D planar structure, which is consistent with previous studies [40]. Figs. 1(d)-1(f) further show the calculated phonon dispersions, which present a strong atomic-mass dependence. A common characteristic among these 2D

materials is the existence of a ZA mode with an ideal quadratic dispersion in the low-frequency region, which is widely recognized to make a significant contribution to TC [21]. It is also noted that the frequencies of phonon modes significantly decrease as the atomic mass  $X$  increases. In particular, the reduction of optical phonon frequencies (TO and LO modes) is generally smaller than that of the acoustical one (LA mode) with  $X$  increasing from B to Ga. Therefore, although h-BN has a negligible phonon band gap between the optical and acoustical modes, both AlN and GaN exhibit sizable band gaps (GaN has the largest gap, i.e., 12 THz). Such remarkable discrepancy in phonon dispersion can induce significant divergence of 4ph processes in the low-temperature region [15,41].

Then we investigate the temperature-dependent TC of the h-XN monolayers. To accomplish this, we adopt the BTE method to obtain the TC of these 2D materials [see Sec. SI in Supplemental Material for details]. This method enables TC calculations to consider various levels of phonon scattering, including 3ph processes at either RTA or ITA levels and the 4ph processes at the RTA level, which can help us effectively distinguish the impact of each phonon scattering process on TC. In order to make a direct comparison of the TC obtained between BTE and MD (it naturally includes 3ph and 4ph processes) methods, we further construct the MLP based on the first-principles calculations, which can be used in both methods. Note that although there have been empirical potentials for the interatomic interactions of h-XN materials, they suffer from a lack of accuracy in comparison to that of MLP [24].

Fig. S1 shows a comprehensive evaluation by comparing forces and energies between DFT and MLP (based on the NEP model [27,31]) calculations. The good consistency of forces and energies shows that our NEP model has a high accuracy in reproducing the potential-energy surface comparable to DFT calculations, which has been demonstrated to ensure accurate predictions of multiple-target physical properties. We additionally calculate the phonon dispersions of h-XN monolayers based on DFT and NEP models. As shown in Fig. 1, phonon dispersion predicted by NEP (red dashed line) shows excellent agreement with that predicted by the DFT calculations (black solid line) for h-XN systems. More importantly, such an excellent consistency is valid

for all phonon modes, including optical phonon modes. These results show that our MLP can accurately describe the harmonic properties of the h-XN monolayers, which is a vital prerequisite to describing the energy and momentum conservation in phonon-phonon scattering processes, enabling an accurate prediction of TC.

Based on our trained MLP, Figs. 2(a)-2(c) show the temperature-dependent TC of h-XN monolayers, calculated using the BTE method. It can be observed that regardless of considering only 3ph scattering or both 3ph and 4ph (denoted as 3+4ph) scatterings, TC of the three monolayers monotonically decreases with temperature increasing from 100 K to 900 K. Note that such monotonic reduction of TC with temperature is consistent with previous studies in the BTE calculations [12,16], which mainly focus on TC at medium and high temperatures. One common feature among these three h-XN monolayers is that a notable reduction of TC can be obtained when the 4ph scattering effect is included, the magnitude of which remarkably increases with the decrease in temperature. Particularly, at 100 K, the reduction of TC reaches up to 37%, 86%, and 67% for BN (from 2612 to 1634 W/mK), AlN (from 454 to 63 W/mK), and GaN (from 131 to 43 W/mK), respectively. These results show the unusually significant 4ph scattering effect on TC of h-XN monolayers, which is unexpected due to the general concept that 4ph processes are unimportant at low temperatures. Furthermore, the observed decrease of TC in BN is obviously less pronounced compared to that of AlN and GaN, showing the strong element-dependence of the 4ph effect. The stronger 4ph effect on TC in AlN and GaN can be attributed to the larger phonon band gap between the optical and acoustical modes, which usually corresponds to the stronger 4ph processes [12].

In Fig. 2(d) we additionally show the temperature-dependent ratio of TC (denoted as  $R_{TC}$ ) from the 3+4ph processes ( $TC_{3+4ph}$ ) to that from 3ph processes ( $TC_{3ph}$ , obtained under ITA), which can effectively illustrate the significance of 4ph scattering on TC. Remarkably, it is found that  $R_{TC}$  remains quite small ( $R_{TC} \leq 0.62$ ) across the whole simulated temperature range for the h-XN monolayers. Moreover,  $R_{TC}$  exhibits a strong dependence on the X element in the XN monolayers. That is, in BN, it remains almost

constant at about 0.6, whereas in AlN and GaN, it initially increases (from 0.14 to 0.3 for AlN, from 0.33 to 0.37 for GaN) and then decreases with increasing temperature from 100 K to 900 K. Note that both two types of variations of  $R_{TC}$  are very different from those in 3D materials, where  $R_{TC}$  monotonically decreases with increasing temperature due to the more pronounced enhancement of 4ph processes [42,43]. To confirm our BTE calculations, we have also calculated the temperature-dependent TC (Fig. S2(a)) and  $R_{TC}$  (Fig. 2d) of bulk silicon (Si). Encouragingly, our results demonstrate a noticeable decrease in the 4ph effect as the temperature decreases, aligning well with previous investigations [12].

To find out the underlying reasons for the reduced TC when considering 4ph processes, we calculate the phonon scattering rates for both 3ph and 4ph processes, which are inversely proportional to TC [34]. Note that here we only focus on the scattering rates in the low-frequency region ( $\omega < 2.5$  THz), where the phonons are expected to be excited at 100 K. Following the general analytical approach [16], we first compare the scattering rates of 3ph at the RTA level (3ph-RTA) and 4ph at the RTA level (4ph-RTA). As shown in Figs. 3(a), the scattering rates of 3ph-RTA are 10-100 times larger than that of 4ph-RTA in 2D BN monolayer with  $\omega < 2.5$  THz, indicating the unimportant role of 4ph-RTA on TC calculations. This result is consistent with general expectations, i.e., it is unnecessary to consider the 4ph processes in low-temperature region [12]. Nonetheless, this approach cannot explain the anomalous phenomena observed in Fig. 2(d), where the BTE results show that 4ph scattering significantly decreases TC for BN even at low temperatures.

It is noticed that recent studies have revealed that the iterative processes of 3ph scattering in 2D materials play an important role in TC calculation in the medium and high temperature regions [41]. Here we further explore iterative processes of 3ph scattering in the low-temperature region. As shown in Figs. 3(a)-3(c), the 3ph scattering rates obtained by using ITA (3ph-ITA) are much smaller than those of 3ph-RTA and become comparable to (or even smaller than) those of 4ph-RTA in the low-frequency region. This result clearly shows that the 4ph scatterings have a significant contribution to the calculated TC under the widely adopted 3+4ph treatment in the low-temperature

region, which explains the unusually small values of  $R_{TC}$  shown in Fig. 2(d). On the other hand, we have conducted similar calculations of scattering rates in bulk Si. It is found that the 3ph scattering rates obtained under ITA are basically identical to those of 3ph-RTA in the low-frequency region, both of them are significantly larger than those of 4ph-RTA (see Fig. S2(b)). This result shows the insignificant contribution of 4ph scattering to the TC of bulk Si, which results in the large  $R_{TC}$  at low temperatures (Fig. 2(d)), being consistent with the general conception [12]. For this type of material, it is sufficient in the conventional approach to only compare 3ph-RTA and 4ph-RTA to evaluate the impact of the 4ph processes on TC.

The above results provide a clear explanation for the anomalously large 4ph effect on TC of 2D materials in the low-temperature region. Especially, in 2D compounds with distinct atomic masses, such as AlN and GaN, the strong 4ph processes under the RTA level can result in a variation of TC over 67% at 100 K. Such a strong 4ph effect stimulates us to further consider whether the RTA is sufficient for the description of TC. Considering that the BTE calculation of 4ph processes meets challenges beyond the RTA level [16], we turn to employing MLP-based MD simulations as a reliable reference [37,44], which can accurately evaluate the TC including all 3ph and 4ph phonon-phonon scatterings. As shown in Figs. 2(a)-2(c), a common feature is that although TC obtained by MD simulations is obviously lower than  $TC_{3ph}$ , it is still much higher than  $TC_{3+4ph}$  in the low-temperature region. This result shows that only considering the 4ph at the RTA level underestimates the TC of 2D materials at low temperatures.

According to the discussions of 3ph scattering, it is reasonable to expect the distinguished iterative processes in 4ph scattering as well. Since it is hard to provide a direct ITA solution for 4ph scattering, here we evaluate the impact of ITA on 4ph scattering by evaluating the relative intensity of phonon normal (N)/Umklapp (U) processes under the RTA level in the BTE calculations. In general, if the N processes are much weaker than the U processes, the accuracy of TC can be acceptable without further employing ITA [45]. In Figs. 4(a)-4(c), we present the 4ph scattering rates of U and N processes for XN monolayers at 100 K. It is worth noting that the scattering rates

of N processes are significantly larger than those of U processes in the low-frequency region for all three 2D materials. This observation is in contrast to the behavior in bulk Si, where the U processes exhibit larger scattering rates than the N processes (see Fig. 4(d)). This result verifies that only considering the 4ph at the RTA level is insufficient for calculating TC of 2D materials at low temperatures, and the inclusion of iterative processes becomes necessary.

Now we further explore the underlying mechanism for the unusually large 4ph effect on TC of 2D materials in the low-temperature region. As indicated in Fig. 1, the low-frequency phonons ( $\omega < 2.5$  THz) are dominated by the three acoustic modes, namely, transverse acoustic (TA), longitudinal acoustic (LA), and ZA modes. In Figs. 3(d)-3(f), we plot the ratio of scattering rates (denoted as  $R_s$ ) between 3+4ph processes and 3ph-ITA processes for these three acoustic modes, the value of which is related to the intensity of 4ph scattering under RTA level. It can be seen that in all the XN monolayers, the  $R_s$  of ZA mode is obviously larger than 1.0 and significantly surpass that of LA and TA modes (especially for AlN and GaN). This feature indicates that the unusually large 4ph scattering processes in the low-frequency region mainly come from the ZA mode, which is a distinctive characteristic exclusive to 2D materials. It is worth noting that the ZA mode in AlN/BN has the largest/smallest  $R_s$  value, showing the most significant/insignificant 4ph processes in the AlN/BN monolayer. This result is consistent with the variation of  $R_{TC}$  with element X in the h-XN monolayers discussed above. On the other hand, we have also calculated  $R_s$  of the three acoustic modes (LA, TA1, TA2) in the bulk Si and found all of them have  $R_s$  around 1.0 in the low-frequency region, showing the insignificant 4ph processes in 3D materials [Fig. S2(c)].

The strong correlation between the 4ph processes and the ZA phonon mode offers a promising avenue for effective manipulation of TC in 2D materials, for example, through the application of tensile strain. Here we adopt the AlN monolayer as an illustration. Fig. 5(a) presents the calculated phonon dispersion of the AlN under a small in-plane tensile strain of 1%. As one can see, the ZA mode exhibits an obvious upshift under the tensile strain, while the LA and TA modes show minimal changes. This result shows that ZA mode is much more sensitive to the tensile strain compared to LA and

TA modes. Fig. 5(b) additionally displays the phonon scattering rates of 3ph-ITA and 4ph-RTA processes with and without the presence of strain. A common feature is that both of them have a sizable decrease in the low-frequency region, owing to the upshift of ZA mode induced by tensile strain. Nonetheless, the 4ph-RTA processes exhibit a much more remarkable decrease in scattering rates than that of 3ph-ITA processes, indicating the greater sensitivity to the variation of ZA mode. The calculated temperature-dependent TC with and without strain is further shown in Fig. 5(c). A noteworthy increase of TC under both 3ph-ITA and 3+4ph scatterings has been obtained when a 1% tensile strain is applied. Particularly, at the low temperature of 100 K, the increment of TC considering 3+4ph scattering (by orders of magnitude) is much more significant than that considering only 3ph-ITA scattering (by a few times). This feature results in a substantial enhancement of  $R_{TC}$  in the low-temperature region as shown in Fig. 5(d). The above results provide clear evidence that the TC of 2D materials in the low-temperature region can be effectively modulated due to the strong correlation between 4ph processes and the ZA mode.

In summary, based on the study combining first-principles calculations, ML techniques, BTE, and MD methods, we have unveiled the unusually strong 4ph processes on low-temperature TC of the 2D materials with ZA phonon mode (i.e., h-XN (X=B, Al, Ga)). We have found that the anomalously strong 4ph processes originate from the ZA phonon mode that uniquely exists in 2D materials. The low-frequency nature of ZA phonon mode makes 4ph processes have remarkable influence on the low-temperature TC. We have also found the significant N processes of 4ph scattering in 2D materials, which make the conventionally adopted perturbation methods for TC calculation insufficient at low temperatures. Furthermore, we have shown that the intensity of 4ph scattering and thus TC can be effectively manipulated through strain engineering, which changes the dispersion of the ZA phonon mode. Our findings provide an avenue for studies on high-order phonon interactions of 2D materials in low-temperature region.

We acknowledge financial support from the Ministry of Science and Technology

of the People's Republic of China (Grant No. 2022YFA1402901) and the Natural Science Foundation of China (Grant No. 12074301).

## References

- [1] M. J. Lee *et al.*, Nat. Commun. **7**, 12011 (2016).
- [2] A. A. Balandin, S. Ghosh, W. Bao, I. Calizo, D. Teweldebrhan, F. Miao, and C. N. Lau, Nano Lett. **8**, 902 (2008).
- [3] Z. Guo, D. Zhang, and X. G. Gong, Appl. Phys. Lett. **95**, 163103 (2009).
- [4] H. F. Feng, B. Liu, and Z. X. Guo, Phys. Rev. B **108**, L241405 (2023).
- [5] B. Mortazavi, E. V. Podryabinkin, I. S. Novikov, S. Roche, T. Rabczuk, X. Y. Zhuang, and A. V. Shapeev, J. Phys.: Mater. **3**, 021t02 (2020).
- [6] X. K. Gu, Z. Y. Fan, and H. Bao, J. Appl. Phys. **130**, 210902 (2021).
- [7] K. Esfarjani, G. Chen, and H. T. Stokes, Phys. Rev. B **84**, 085204 (2011).
- [8] A. Seko, A. Togo, H. Hayashi, K. Tsuda, L. Chaput, and I. Tanaka, Phys. Rev. Lett. **115**, 205901 (2015).
- [9] A. J. H. McGaughey, A. Jain, H.-Y. Kim, and B. Fu, J. Appl. Phys. **125**, 011101 (2019).
- [10] L. Lindsay, C. Hua, X. L. Ruan, and S. Lee, Mater. Today Phys. **7**, 106 (2018).
- [11] T. L. Feng and X. L. Ruan, Phys. Rev. B **97**, 045202 (2018).
- [12] T. Feng, L. Lindsay, and X. Ruan, Phys. Rev. B **96**, 161201(R) (2017).
- [13] X. L. Yang, T. L. Feng, J. Li, and X. L. Ruan, Phys. Rev. B **100**, 245203 (2019).
- [14] X. K. Gu, Z. Y. Fan, H. Bao, and C. Y. Zhao, Phys. Rev. B **100**, 064306 (2019).
- [15] S. T. Ning, S. Huang, T. T. Zhang, Z. Y. Zhang, N. Qi, and Z. Q. Chen, J. Phys. Chem. C **126**, 17885 (2022).
- [16] Z. R. Han, X. L. Yang, W. Li, T. L. Feng, and X. L. Ruan, Comput. Phys. Commun. **270**, 108179 (2022).
- [17] J. S. Kang, M. Li, H. A. Wu, H. Nguyen, and Y. J. Hu, Science **361**, 575 (2018).
- [18] S. Li, Q. Y. Zheng, Y. C. Lv, X. Y. Liu, X. Q. Wang, P. Huang, D. G. Cahill, and B. Lv, Science **361**, 579 (2018).
- [19] Z. C. Liu, X. L. Yang, B. Zhang, and W. Li, ACS Appl. Mater. Interfaces **13**, 53409 (2021).
- [20] L. Lindsay, W. Li, J. Carrete, N. Mingo, D. A. Broido, and T. L. Reinecke, Phys. Rev. B **89**, 155426 (2014).
- [21] L. Lindsay, D. A. Broido, and N. Mingo, Phys. Rev. B **82**, 115427 (2010).
- [22] Y. L. Ouyang, C. Q. Yu, J. He, P. F. Jiang, W. J. Ren, and J. Chen, Phys. Rev. B **105**, 115202 (2022).
- [23] K. Xu *et al.*, Phys. Rev. B **99**, 054303 (2019).
- [24] B. Mortazavi, E. V. Podryabinkin, I. S. Novikov, T. Rabczuk, X. Y. Zhuang, and A. V. Shapeev, Comput. Phys. Commun. **258**, 107583 (2021).
- [25] Y. Mishin, Acta Mater. **214**, 116980 (2021).
- [26] O. T. Unke, S. Chmiela, H. E. Sauceda, M. Gastegger, I. Poltaysky, K. T. Schütt, A. Tkatchenko, and K. R. Müller, Chem. Rev. **121**, 10142 (2021).
- [27] Z. Fan, Z. Zeng, C. Zhang, Y. Wang, K. Song, H. Dong, Y. Chen, and T. Ala-Nissila, Phys. Rev. B **104**, 104309 (2021).

- [28] G. Kresse and J. Furthmuller, *Comput. Mater. Sci* **6**, 15 (1996).
- [29] J. P. Perdew, K. Burke, and M. Ernzerhof, *Phys. Rev. Lett.* **77**, 3865 (1996).
- [30] G. Kresse and D. Joubert, *Phys. Rev. B* **59**, 1758 (1999).
- [31] D. Wierstra, T. Schaul, T. Glasmachers, Y. Sun, J. Peters, and J. Schmidhuber, *J. Mach. Learn. Res.* **15**, 949 (2014).
- [32] Z. Y. Fan, *J. Phys.: Condens. Matter* **34**, 125902 (2022).
- [33] J. Behler, *J. Chem. Phys.* **145**, 170901 (2016).
- [34] W. Li, J. Carrete, N. A. Katcho, and N. Mingo, *Comput. Phys. Commun.* **185**, 1747 (2014).
- [35] D. A. Broido, M. Malorny, G. Birner, N. Mingo, and D. A. Stewart, *Appl. Phys. Lett.* **91**, 231922 (2007).
- [36] A. Ward, D. A. Broido, D. A. Stewart, and G. Deinzer, *Phys. Rev. B* **80**, 125203 (2009).
- [37] Z. Y. Fan *et al.*, *J. Chem. Phys.* **157**, 114801 (2022).
- [38] W. G. Hoover, *Phys. Rev. A* **31**, 1695 (1985).
- [39] J. Tersoff, *Phys. Rev. B* **39**, 5566 (1989).
- [40] T. Kocabas, M. Keçeli, A. Vázquez-Mayagoitia, and C. Sevik, *Nanoscale* **15**, 8772 (2023).
- [41] S. P. Bi, Z. Chang, K. P. Yuan, Z. H. Sun, X. L. Zhang, Y. F. Gao, and D. W. Tang, *J. Appl. Phys.* **132**, 114301 (2022).
- [42] X. Gu, S. Li, and H. Bao, *Int. J. Heat Mass Transfer* **160**, 120165 (2020).
- [43] B. Zhang, Z. Y. Fan, C. Y. Zhao, and X. K. Gu, *J. Phys.: Condens. Matter* **33**, 495901 (2021).
- [44] Z. Y. Fan, W. Chen, V. Vierimaa, and A. Harju, *Comput. Phys. Commun.* **218**, 10 (2017).
- [45] A. Ward and D. A. Broido, *Phys. Rev. B* **81**, 085205 (2010).

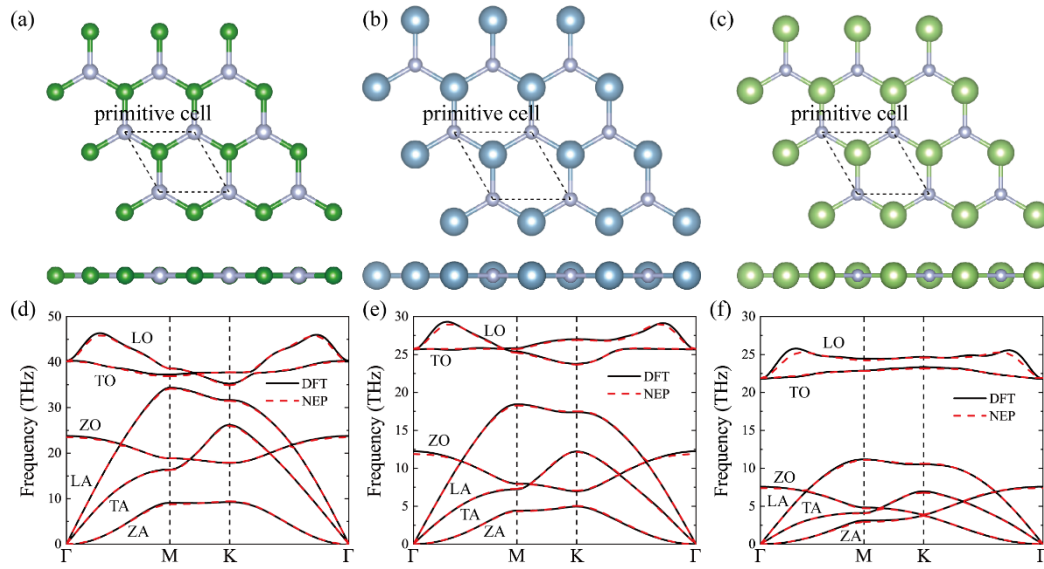


Fig. 1. (a)-(c): Top and side views of optimized monolayer (a) h-BN, (b) h-AlN, and (c) h-GaN. The green balls represent B atoms, the blue balls represent Al atoms, the light green balls represent Ga atoms, and the grey balls represent N atoms. (d)-(f): Phonon dispersions of (d) h-BN, (e) h-AlN, and (f) h-GaN along the high-symmetry paths. The solid lines and dashed lines are the results from DFT and NEP, respectively.

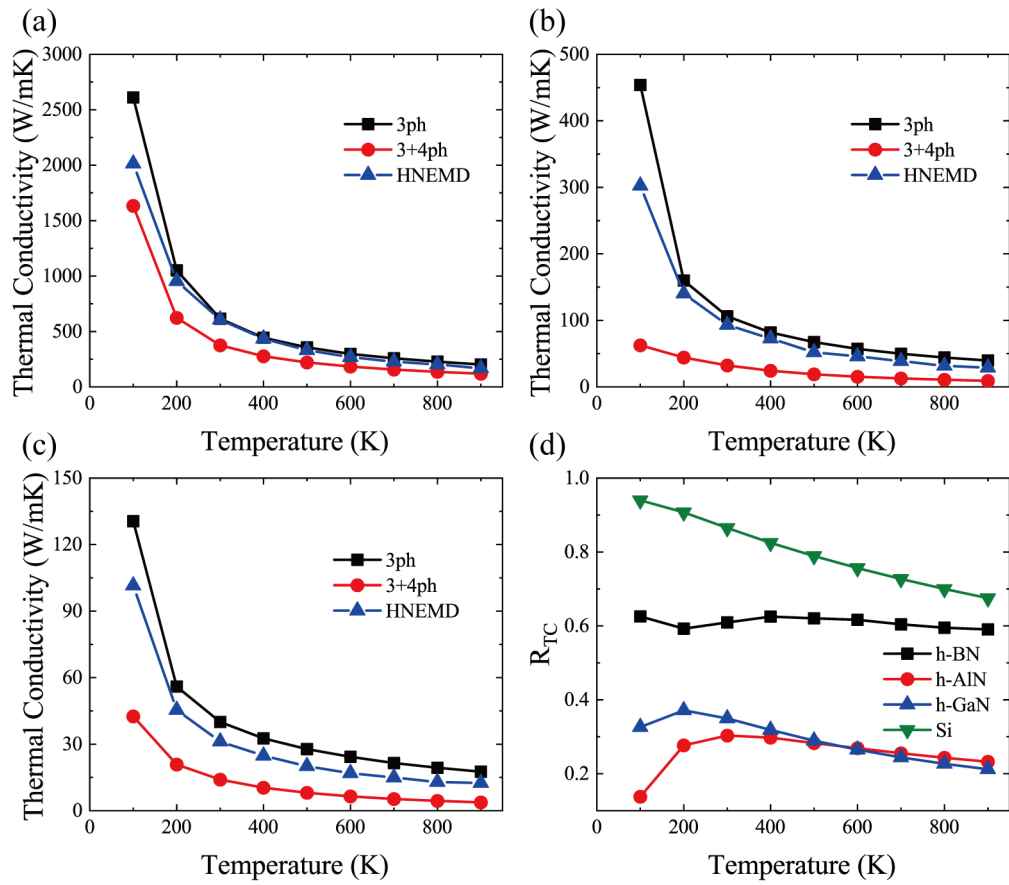


Fig. 2. Thermal conductivity of (a) h-BN, (b) h-AlN, and (c) h-GaN as a function of temperature. (d) The ratio of TC (denoted as  $R_{TC}$ ) obtained from 3+4ph processes to that from 3ph processes, for h-XN monolayers and bulk Si.

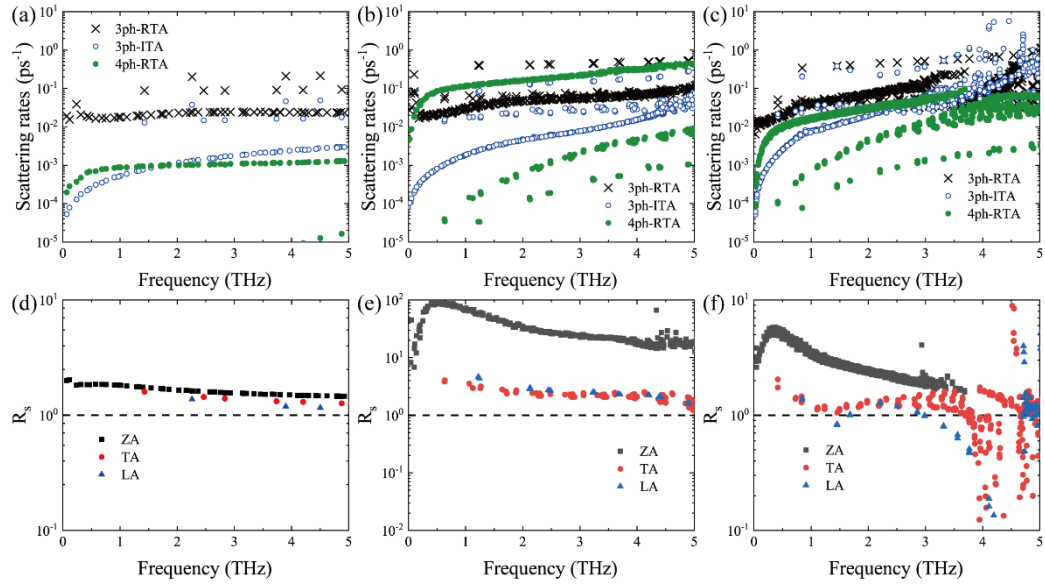


Fig. 3. (a)-(c): Scattering rates at 100 K of 3ph-RTA, 4ph-RTA, 3ph-ITA, and 3+4ph-ITA for (a) h-BN, (b) h-AlN, and (c) h-GaN, respectively. (d)-(f): The corresponding ratio of scattering rates (denoted as  $R_s$ ) between 3+4ph and 3ph-ITA processes for (d) h-BN, (e) h-AlN, and (f) h-GaN, respectively.

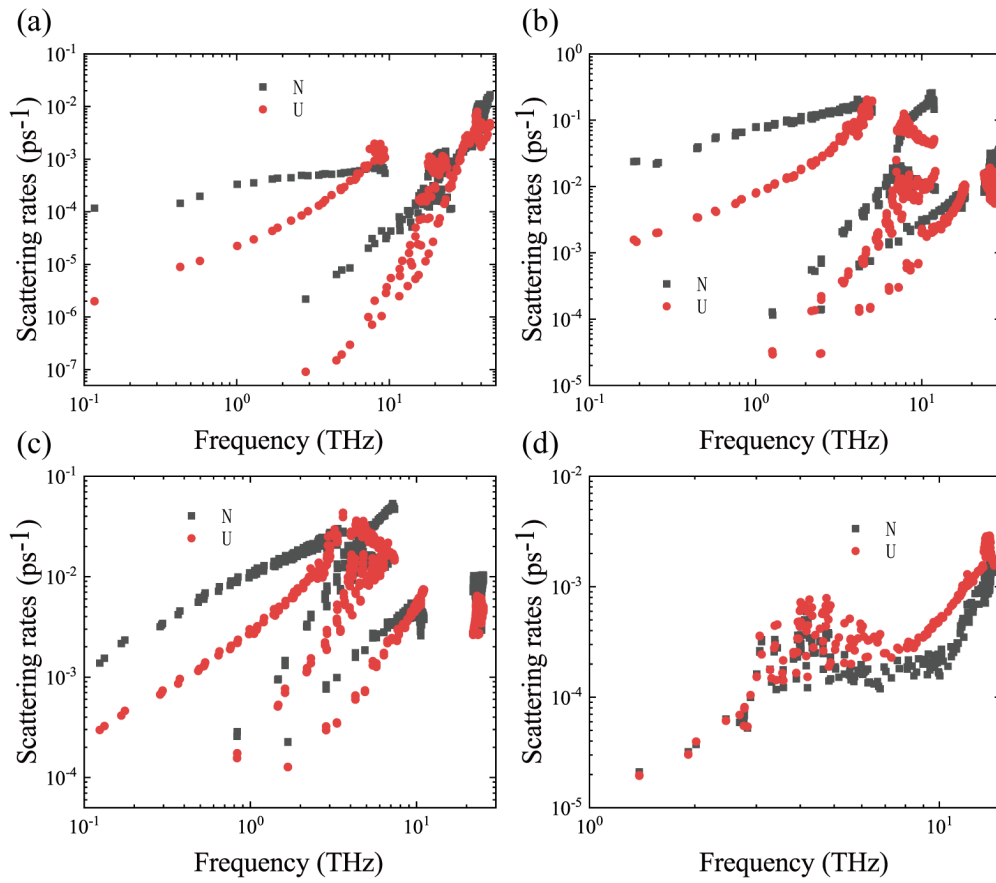


Fig. 4. The 4ph scattering rates of N and U processes at 100 K for (a) h-BN, (b) h-AlN, (c) h-GaN, and (d) bulk Si, respectively.

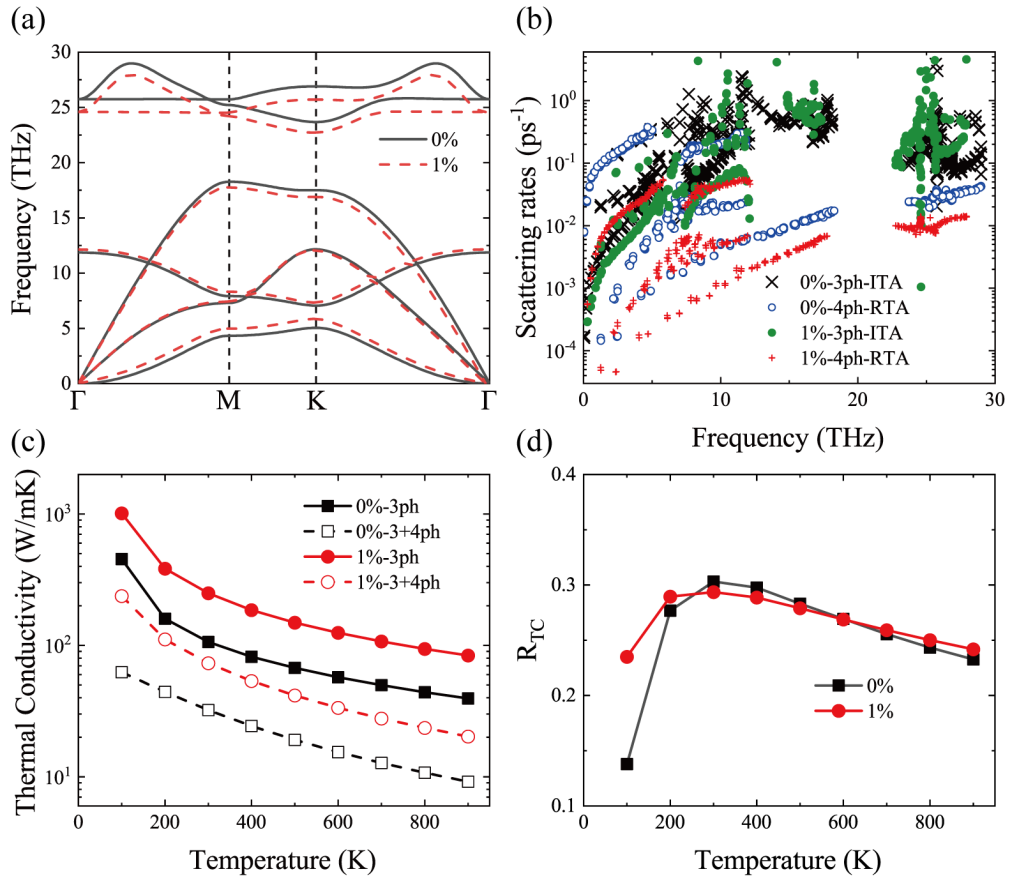


Fig. 5. Comparison of results obtained with and without tensile strain in h-AlN monolayer. (a) The phonon dispersion curves. (b) Scattering rates of 3ph-ITA and 4ph-RTA. (c) TC of 3ph (from the scattering rates of 3ph-ITA) and 3+4ph processes as a function of temperature. (d) The ratio of TC obtained from the 3+4ph processes to that from the 3ph processes.